ELSEVIER

Journal of Biomechanics 39 (2006) 177–183

JOURNAL OF BIOMECHANICS

www.elsevier.com/locate/jbiomech
www.JBiomech.com

Short communication

A numerical method for the continuous spectrum biphasic poroviscoelastic model of articular cartilage

Mansoor A. Haider*, Richard C. Schugart

Department of Mathematics, North Carolina State University, Box 8205, Raleigh, NC 27695-8205, USA

Accepted 13 October 2004

Abstract

A method for numerical solution of the continuous spectrum linear biphasic poroviscoelastic (BPVE) model of articular cartilage is presented. The method is based on an alternate formulation of the continuous spectrum stress–strain law that is implemented using Gaussian quadrature integration combined with quadratic interpolation of the strain history. For N time steps, the cost of the method is $O(N)$. The method is applied to a finite difference solution of the one-dimensionsal confined compression BPVE stress-relaxation problem. For a range of relaxation times that are representative of articular cartilage, accuracy of the method is demonstrated by direct comparison to a theoretical Laplace transform solution.

Keywords: Biphasic poroviscoelastic model; Articular cartilage; Stress relaxation; Numerical method

1. Introduction

The linear biphasic poroviscoelastic (BPVE) model of articular cartilage (Mak, 1986) has been used to describe tissue deformation resulting from a combination of inter-phase (flow-dependent) and intrinsic (flow-independent) dissipation mechanisms. Intrinsic dissipation in cartilage has been modeled using a constitutive law in which the solid matrix stress depends on the strain-rate via a hereditary integral with a continuous relaxation spectrum (Fung, 1993). Several investigators have used BPVE models to measure viscoelastic parameters in cartilage explants (DiSilvestro and Suh, 2001, 2002; Setton et al., 1993). To overcome the prohibitive cost of evaluating the hereditary stress–strain integral in fixed step integration schemes, it is common to use a discrete spectrum approximation of the continuous spectrum relaxation function in terms of an exponential series. The discrete spectrum approximation has been incorporated into a biphasic finite element method (FEM) to develop an efficient computational BPVE model (Suh and Bai, 1998). Notably, this discrete spectrum BPVE model was employed in a cross-validation study in which bovine cartilage parameters were measured, simultaneously, in three independent loading configurations (DiSilvestro and Suh, 2001). While the primary advantage of the BPVE model under consideration is the incorporation of intrinsic viscoelasticity in the solid phase, it is noted that this model neglects anisotropic and nonlinear behavior of articular cartilage.

In the discrete spectrum BPVE model a new set of viscoelastic parameters, written in terms of the three parameters in the continuous spectrum relaxation function, is introduced via an exponential series approximation. While this approximation facilitates implementation of an efficient numerical method (Suh and Bai, 1998), the dependence of the new parameters on the three original parameters is chosen arbitrarily and therefore non-unique. In this study, we present a numerical method that can significantly accelerate evaluation of the continuous spectrum BPVE model without the need to introduce an exponential series

*Corresponding author. Tel.: +1 919 515 3100; fax: +1 919 515 3798.
E-mail address: m_haider@ncsu.edu (M.A. Haider).

0021-9290/$ - see front matter © 2004 Elsevier Ltd. All rights reserved.
doi:10.1016/j.jbiomech.2004.10.037

approximation. Our method is based on an alternate formulation of the continuous spectrum constitutive law that is implemented using Gaussian quadrature time integration in combination with quadratic interpolation of the strain history. The accuracy and cost of this method are evaluated using a finite difference solution of the one-dimensional (1D) confined compression stress-relaxation problem for ranges of long- and short-term relaxation times that are representative of articular cartilage.

2. Methods

We present an alternative to fixed step time integration schemes for the BPVE model. The potential benefits of the proposed scheme are illustrated via a finite difference numerical solution of the one-dimensional (1D) confined compression stress relaxation problem in small strain, where an analytical Laplace transform solution is available for comparison (Mak, 1986).

In the 1D BPVE model, the reduced momentum equation is

$$\frac{\partial \sigma}{\partial z} = \frac{1}{\kappa}\frac{\partial u}{\partial t}, \quad 0<z<h, \;\; 0<t<t_\infty, \tag{1}$$

where $u(z,t)$ is the axial (z) displacement, h is the sample size, κ is the hydraulic permeability and t_∞ is the duration of the experiment. The solid matrix stress σ is viscoelastic and of the form (e.g. Setton et al., 1993):

$$\sigma(z,t) = H_A \int_{-\infty}^{t} G(t-\tau)\frac{\partial}{\partial \tau}\left(\frac{\partial u}{\partial z}(z,\tau)\right)\mathrm{d}\tau, \tag{2}$$

where H_A is the "drained" aggregate modulus of the solid phase. We consider the case where both deviatoric and dilatational stress relaxation are governed by a single continuous spectrum relaxation function, of the form suggested by Fung (1993), (Neubert, 1963)

$$G(t) = 1 + c\int_{\tau_1}^{\tau_2}\frac{\mathrm{e}^{-t/\tau}}{\tau}\,\mathrm{d}\tau = 1 + c\left[E_1\left(\frac{t}{\tau_2}\right) - E_1\left(\frac{t}{\tau_1}\right)\right], \tag{3}$$

where $E_1(z)$ is the exponential integral function.

2.1. Alternate formulation

The governing equations (1)–(2) are nondimensionalized via the transformation $u = h\bar{u}, \sigma = H_A\bar{\sigma}, z = h\bar{z}$ and $t = t_C\bar{t}$, where $t_C = h^2/(\kappa H_A)$ is the biphasic gel relaxation time (Mow et al., 1980). Assuming that $\bar{u}(\bar{z},\bar{t}) = 0$ for $\bar{t}<0$, our alternate formulation is based on integration of relation (2), by parts. It is straightforward to show that the nondimensional governing equation (1) reduces to $\partial\bar{\sigma}/\partial\bar{z} = \partial\bar{u}/\partial\bar{t}$ $(0<\bar{z}<1, 0<\bar{t}<\bar{t}_\infty)$ where

$$\bar{\sigma}(\bar{z},\bar{t}) = \left[1 + c\log\left(\frac{\tau_2}{\tau_1}\right)\right]\varepsilon(\bar{z},\bar{t}) - c\int_0^{\bar{t}} H(\bar{t}-\bar{\tau})\varepsilon(\bar{z},\bar{\tau})\,\mathrm{d}\bar{\tau}, \tag{4}$$

$\varepsilon = \partial u/\partial z$ is the strain, and the modified kernel in the integral is

$$H(s) = \frac{\mathrm{e}^{-s/\bar{\tau}_2} - \mathrm{e}^{-s/\bar{\tau}_1}}{s} \quad (s = \bar{t} - \bar{\tau}). \tag{5}$$

The numerical method is based on the following two observations regarding the alternate formulation (4) of the stress–strain relation:

1. In contrast to the relaxation function G in (3), the modified kernel H is explicit and exhibits a two-scale structure in s that can be used to accurately integrate (4) using Gaussian quadrature. The time-stepping algorithm for numerical solution of the governing equation (1) can be uncoupled from the numerical integration used to update the stress (4) via interpolation of the strain history. The result is a significant cost reduction as compared to schemes that employ a fixed step time integration of (2) (e.g. using Simpson's rule).
2. In small (or finite) strain models, the strain history in (4) is assumed to be bounded by a maximum strain $\varepsilon_{\max}$ in space and time. Consequently, evaluation of the integral in (4) can be truncated at a critical relative time $s_c = \bar{t} - \bar{t}_c$ that is given by the error estimate

$$c\varepsilon_{\max}\left|\int_{s_c}^{t} H(s)\,\mathrm{d}s\right| < c\varepsilon_{\max}\left|E_1\left(\frac{s_c}{\bar{\tau}_2}\right) - E_1\left(\frac{s_c}{\bar{\tau}_1}\right)\right| < c\varepsilon_{\max}\left|E_1\left(\frac{s_c}{\bar{\tau}_2}\right)\right| = \mathrm{TOL}, \tag{6}$$

where TOL determines accuracy of the truncated approximation and the properties $\tau_1<\tau_2$ and $E_1(s)>E_1(t)$ (for $0<s<t$) have been used. Truncation via this error estimate can significantly reduce storage requirements for the strain history when $t_\infty \gg \tau_2$.

The primary benefit of the alternate formulation (4) is item 1 which, for N time steps, reduces the cost of evaluating the hereditary integral from $O(N^2)$ to $O(N)$. The slope of the linear cost curve is determined by the number of quadrature points required to accurately approximate the integral. The required number of quadrature points increases as $\tau_1 \to 0$, since τ_1 governs the size of the boundary layer in $H(s)$ for small s. The cost and memory requirements of this approach are greater than those associated with methods based on a discrete spectrum approximation of (2) (Suh and Bai, 1998), but significantly less than costs for the fixed time

step $O(N^2)$ method. The proposed continuous spectrum method produces results nearly identical to those of the $O(N^2)$ method without the need to re-approximate the relaxation function using an exponential series.

2.2. Implementation

To assess accuracy of the proposed numerical method, we consider a finite-difference solution of (1) based on the alternate formulation (4) and the error estimate (6). Define a spatial grid $\bar{z}_j = j\Delta\bar{z}$ ($j = 0,\ldots,M, \Delta\bar{z} = 1/M$), a time step $\Delta\bar{t}$ with $\bar{t}_k = k\Delta\bar{t}$ ($k = 0,\ldots,N, \Delta t = t_\infty/N$), and let $(\cdot)_j^k = (\cdot)(\bar{z}_j, \bar{t}_k)$. At time $\bar{t} = \bar{t}_k$, the nondimensional momentum equation is discretized using an (implicit) backward difference scheme in both space and time

$$\frac{\bar{u}_j^k - \bar{u}_j^{k-1}}{\Delta\bar{t}} = \frac{\bar{\sigma}_j^k - \bar{\sigma}_{j-1}^k}{\Delta\bar{z}}, \quad j = 1,\ldots,M. \tag{7}$$

The strain $\varepsilon = \partial u/\partial z$ is discretized using a forward difference in space $\varepsilon_j^k \approx D^+\bar{u}_j^k = (\bar{u}_{j+1}^k - \bar{u}_j^k)/(\Delta\bar{z})$. Consider the first stress term on the right-hand side of (7). Using (4), write

$$\bar{\sigma}_j^k = \left[1 + c\log\left(\frac{\tau_2}{\tau_1}\right)\right] D^+\bar{u}_j^k - c\int_0^{\bar{t}^k} H(\bar{t}^k - \bar{\tau}) \times \varepsilon(\bar{z}_j, \bar{\tau})\,\mathrm{d}\bar{\tau}, \quad j = 1,\ldots,M-1. \tag{8}$$

Motivated by the aforementioned properties of the kernel H, the numerical integration scheme is based on writing (8) as

$$\bar{\sigma}_j^k = \left[1 + c\log\left(\frac{\tau_2}{\tau_1}\right)\right] D^+\bar{u}_j^k - c\int_{\max(0,\bar{t}^k - s_c)}^{\bar{t}^k} H(\bar{t}^k - \bar{\tau}) \times \varepsilon(\bar{z}_j, \bar{\tau})\,\mathrm{d}\bar{\tau} - c\int_{\bar{t}^*}^{\bar{t}^k} H(\bar{t}^k - \bar{\tau})\varepsilon(\bar{z}_j, \bar{\tau})\,\mathrm{d}\bar{\tau}, \tag{9}$$

where s_c is determined from (6), and the choice $\bar{t}^* = 10\bar{\tau}_1$ facilitates accurate integration of the boundary layer in $H(s)$ near $s = 0$. Applying regular Gaussian quadrature to the integrals in (9)

$$\bar{\sigma}_j^k = \left[1 + c\log\left(\frac{\tau_2}{\tau_1}\right)\right] D^+\bar{u}_j^k - c\sum_{l=1}^{N_q^{(2)}} \eta_l H(\bar{t}^k - \bar{\alpha}_l)\varepsilon(\bar{z}_j, \bar{\alpha}_l) - c\sum_{l=1}^{N_q^{(1)}} \gamma_l H(\bar{t}^k - \bar{\beta}_l)\varepsilon(\bar{z}_j, \bar{\beta}_l), \tag{10}$$

where $\eta_l, \bar{\alpha}_l$ are weights and abcissas for $N_q^{(2)}$-point Gaussian quadrature on the interval $[\max(0, \bar{t}^k - s_c), \bar{t}^*]$, and $\gamma_l, \bar{\beta}_l$ are weights and abcissas for $N_q^{(1)}$-point Gaussian quadrature on the interval $[\bar{t}^*, \bar{t}^k]$ (for values see Section 25.4.30, Abramowitz and Stegun, 1972). In cases where τ_1 is relatively large, the intermediate point $\bar{t}^*$ is not required and a single quadrature integration on the interval $[\max(0, \bar{t}^k - s_c), \bar{t}^k]$ is sufficient for accurate numerical integration.

Evaluation of (10) requires knowledge of the strain history ε at times corresponding to the abcissas, which do not coincide with the times $\bar{t}^k$ ($k = 1,\ldots,N$) in the (time marching) finite difference scheme. Strains at intermediate times are approximated using quadratic interpolation of strain values at the fixed step times. The following numerical integration scheme is proposed:

1. At the first step of the finite difference solution ($k = 1$), (8) is integrated using the trapezoidal rule
$$\bar{\sigma}_j^1 = \left[1 + c\log\left(\frac{\tau_2}{\tau_1}\right)\right] D^+\bar{u}_j^1 - \frac{c\Delta\bar{t}}{2}\left(H(\Delta\bar{t})\varepsilon(\bar{z}_j, 0) + H(0)D^+\bar{u}_j^1\right). \tag{11}$$

2. At the second step of the finite difference solution ($k = 2$), (8) is integrated using Simpson's rule
$$\bar{\sigma}_j^2 = \left[1 + c\log\left(\frac{\tau_2}{\tau_1}\right)\right] D^+\bar{u}_j^2 - \frac{c\Delta\bar{t}}{3}\left(H(2\Delta\bar{t})\varepsilon(\bar{z}_j, 0) + 4H(\Delta\bar{t})D^+\bar{u}_j^1 + H(0)D^+\bar{u}_j^2\right). \tag{12}$$

3. For $k \geqslant 3$,the strain at an intermediate time $\bar{\alpha}_l$ is evaluated by locating the interval with $\bar{\alpha}_l \in (\bar{t}^m, \bar{t}^{m+1})$ via a simple coordinate transformation. Using the known strain values $\varepsilon_j^{m-1}, \varepsilon_j^m$ and ε_j^{m+1},a quadratic interpolation of the strain is constructed and used to approximate $\varepsilon(\bar{z}_j, \bar{\alpha}_l)$. In the case $m + 1 = k$,ε_j^{m+1} is not known and the strain values $\varepsilon_j^{m-2}, \varepsilon_j^{m-1}$ and ε_j^m are used to construct a quadratic interpolation which is extrapolated to evaluate $\varepsilon(\bar{z}_j, \bar{\alpha}_l)$. Via this interpolation scheme, the quadrature sums in (10) are evaluated. Note that in the early time region $\bar{t}^k < 10\bar{\tau}_1$, the intermediate point$\bar{t}^*$ is not used and only one quadrature integral is evaluated on the interval $[\max(0, \bar{t}^k - s_c), \bar{t}^k]$.

The stress representations obtained using (10)–(12) are substituted into (7) to obtain an implicit finite difference scheme for the unknown displacements that is first-order accurate in time and second-order accurate in space. For N time steps, the cost of numerical integration is roughly $(N_q^{(1)} + N_q^{(2)})N$, where $N_q^{(1)}$ and $N_q^{(2)}$ depend on the orders of magnitude of τ_1 and τ_2. For large N, the storage requirements of this numerical method are not greater than $s_c/\Delta t M$ and will provide significant savings over the storage requirements associated with integration of the full strain history, which are NM, when $\tau_2 \ll t_\infty$.

3. Results

Based on the literature for application of the BPVE model to articular cartilage, viscoelastic relaxation times were considered for the cases $\tau_1 = 0.01,\ 0.1,\ 1.0$ s and $\tau_2 = 10, 100, 200$ s, with $c = 1$. Biphasic and geometric parameter values were chosen based on mean parameter values in the cross-validation study of DiSilvestro and Suh (2001) as $E = 0.63$ MPa and $\nu = 0.1$ ($\Rightarrow H_A = 1.29$ MPa), $\kappa = 1.72 \times 10^{-5}\ \mathrm{m}^4/(\mathrm{Ns})$ and $h = 1.28$ mm. In their study, mean short- and long-term relaxation times in the discrete spectrum approximation were found to be 0.62 and 85.1 s, respectively.

The continuous spectrum numerical method was used to simulate the 1D confined compression stress-relaxation problem with a fixed impermeable boundary at $z = h$ and a free-draining boundary at $z = 0$, subject to the prescribed displacements $u(0,t) = v_0 t$ (for $0 \leqslant t \leqslant t_0$), and $u(0,t) = u_0 = v_0 t_0$ (for $t_0 < t \leqslant t_\infty$). In all simulations, the ramp amplitude was $u_0 = h/10$ and the duration of the experiment was chosen to be $t_\infty = 1800$ s. All results were obtained using the values $\varepsilon_{\max} = 0.1, \mathrm{TOL} = 10^{-3}$ in the error estimate (6) and, in demonstrating accuracy of the method, a ramp time of $t_0 = 10$ s was chosen. Computations were performed in MATLAB 6.5 on a dual-1 GHz-processor G4 Power Macintosh. Once the displacement solution was computed using (7) with (10)–(12), the surface stress was calculated using a four-point finite difference approximation $\bar{\sigma}_0^k \approx [1 + c\log(\tau_2/\tau_1)](\frac{1}{3}\bar{u}_3^k - \frac{3}{2}\bar{u}_2^k + 3\bar{u}_1^k - \frac{11}{6}\bar{u}_0^k)/\Delta\bar{z}$ $(k = 1, \ldots, N)$.

Truncation of the strain history in the first integral of (9), using the error estimate (6), is illustrated in Fig. 1 and is insensitive to τ_1. For $\tau_2 = 10$ s, roughly 50 s of the strain history need to be retained. This value increases to roughly 650 s as τ_2 increases to 200 s, representing just over $\frac{1}{3}$ of the duration of the full simulation.

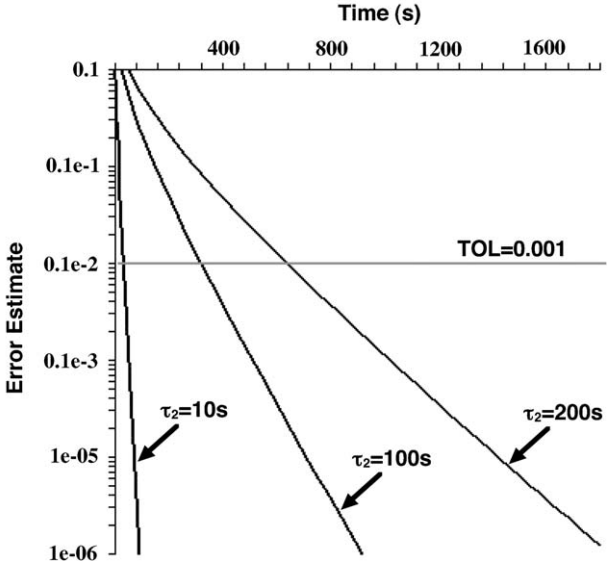

Fig. 1. Graph of the error estimate in (6) with varying long-term relaxation time τ_2.

Performance of the numerical method was assessed by comparison to a theoretical Laplace transform solution of the 1D confined compression stress relaxation problem (Mak, 1986—Eqs. (24)–(25)). Numerical inversion of Laplace transform representations was performed using an implementation (Hollenbeck, 1998) of deHoog's algorithm (deHoog et al., 1982) in MATLAB. To illustrate numerical convergence, the normalized surface stress $\sigma(0,t)/\sigma_\infty$ was compared to the theoretical solution as the order of Gaussian quadrature was increased (Fig. 2a). For the case shown in Fig. 2, accuracy is established at $L = 32$ and the computational cost grows linearly with the number of time steps (Fig. 2b). The slope of the cost curve increases in proportion to the factor by which L is increased. Using the error estimate (6), the effects of truncating the strain history integral on storage requirements in the time marching method are illustrated in Fig. 2c. In contrast to a fixed step integration rule, only a fixed portion of the strain history need be retained once $t > s_c$.

Accuracy of the numerical method was evaluated over the range of relaxation times by comparing computed values of displacement in the layer (Fig. 3a–c) and surface stress (Fig. 3d) to the theoretical solution. The case $\tau_1 = 0.1$ s is shown and the displacement and stress curves are indistinguishable for the cases $\tau_1 = 0.01$, and 1.0 s, since the ramp time $t_0 = 10$ s corresponds to a relatively low strain rate. Table 1 lists the number of quadrature points required to obtain results of comparable accuracy to those shown in Fig. 3 over the full range of relaxation times considered. A mesh of resolution $\Delta\bar{z} = \frac{1}{20}$ and $\Delta\bar{t} = \frac{1}{30}$ was sufficient in all cases listed. To evaluate accuracy of the numerical method in cases where results are sensitive to τ_1, the ramp time was decreased to $t_0 = 0.05$ s. At such (higher) strain rates, τ_1 is distinguished from the early (ramp) response of the surface stress (Fig. 4). Accurate results were obtained for a mesh of resolution $\Delta\bar{z} = \frac{1}{80}$ and $\Delta\bar{t} = \frac{1}{300}$ with one 8-point Gaussian quadrature integration over the full strain history.

4. Discussion

We have presented a $O(N)$ continuous spectrum numerical solution of the BPVE cartilage model that produces results nearly identical to the theoretical solution, and hence also to $O(N^2)$ solutions based on fixed step time integration of the hereditary stress–strain integral. As demonstrated in Fig. 3 and Table 1, accurate results can be obtained with two 32-point quadrature intervals in all but the case $\tau_1 = 0.01$ s, where the number of quadrature points per layer increases to

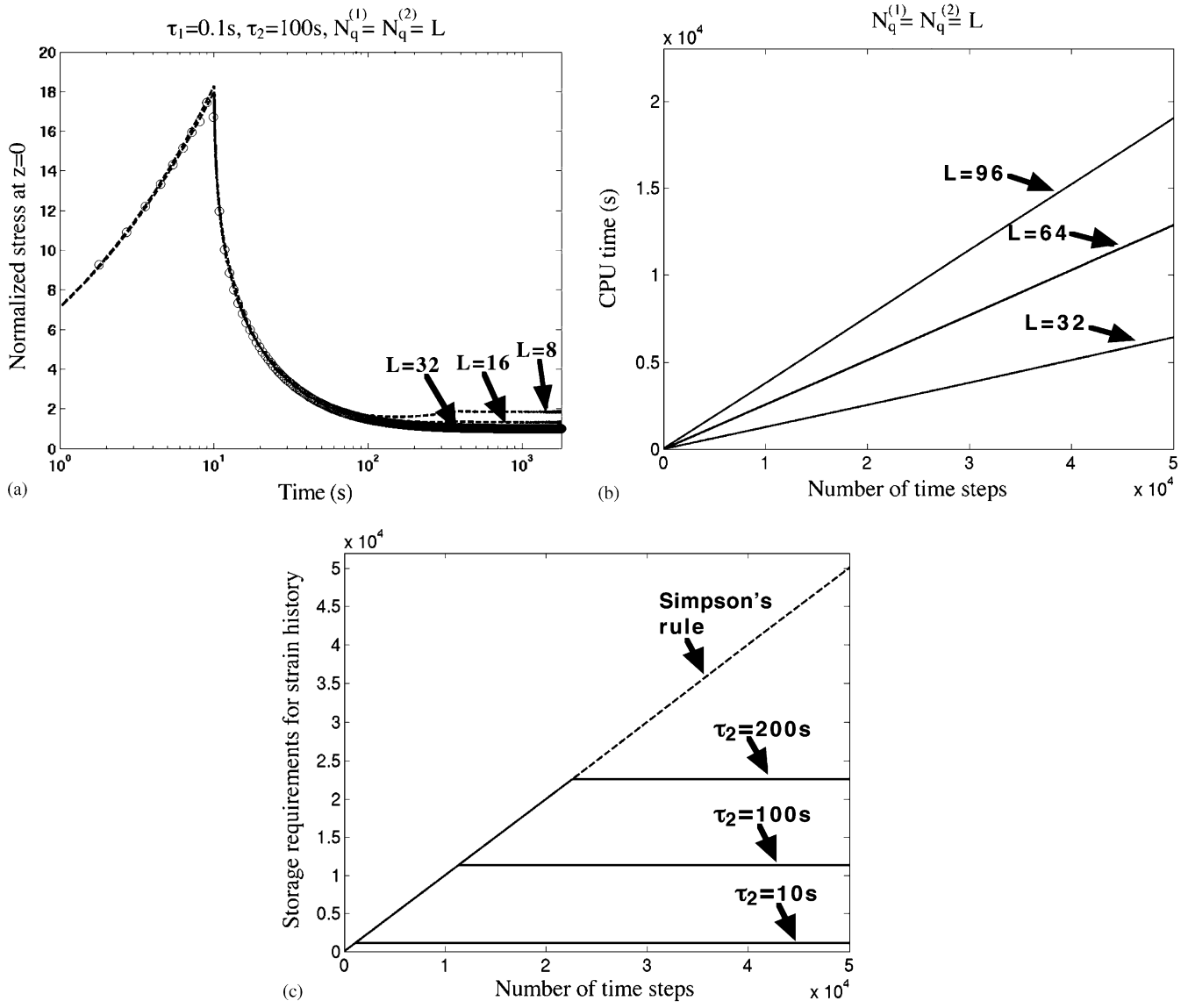

Fig. 2. Performance of the continuous spectrum BPVE numerical method ($\Delta\bar{t} = \frac{1}{30}, \Delta\bar{z} = \frac{1}{20}$): (a) A comparison of the computed surface stress (dashed) with the theoretical solution (circles) as the order of quadrature L is increased. (b) Cost of the numerical method as L is increased. (c) Storage requirements for the strain history as the long-term relaxation time τ_2 is increased.

Table 1
The order of Gaussian quadrature required for accuracy of the numerical method for the range of relaxation times associated with articular cartilage ($\Delta\bar{t} = \frac{1}{30}, \Delta\bar{z} = \frac{1}{20}$)

τ_1	τ_2	$N_q^{(1)}$	$N_q^{(2)}$
1	10	32	32
1	100	32	32
1	200	32	32
0.1	10	32	32
0.1	100	32	32
0.1	200	32	32
0.01	10	32	32
0.01	100	64	64
0.01	200	96	96

96 as τ_2 is increased to 200 s. In the worst case ($L = 96$), the quadrature integration at one spatial point requires the summation of roughly $192N$ values for N time steps, while a fixed step method would require the summation of roughly $N(N+1)/2$ values. For $\Delta t = \frac{1}{30}$ and $t_\infty = 1800$ s, $N = 54,000$ and the cost difference is very large.

The BPVE FEM (Suh and Bai, 1998) is based on a recursive relation for the hereditary integral that requires retention of strain history only locally in time. However, since their method is based on a discrete spectrum approximation of the continuous spectrum relaxation function, it requires the introduction of a somewhat arbitrary set of alternate parameters that are non-unique, a constraint that is not present in our approach. The numerical method presented in this study

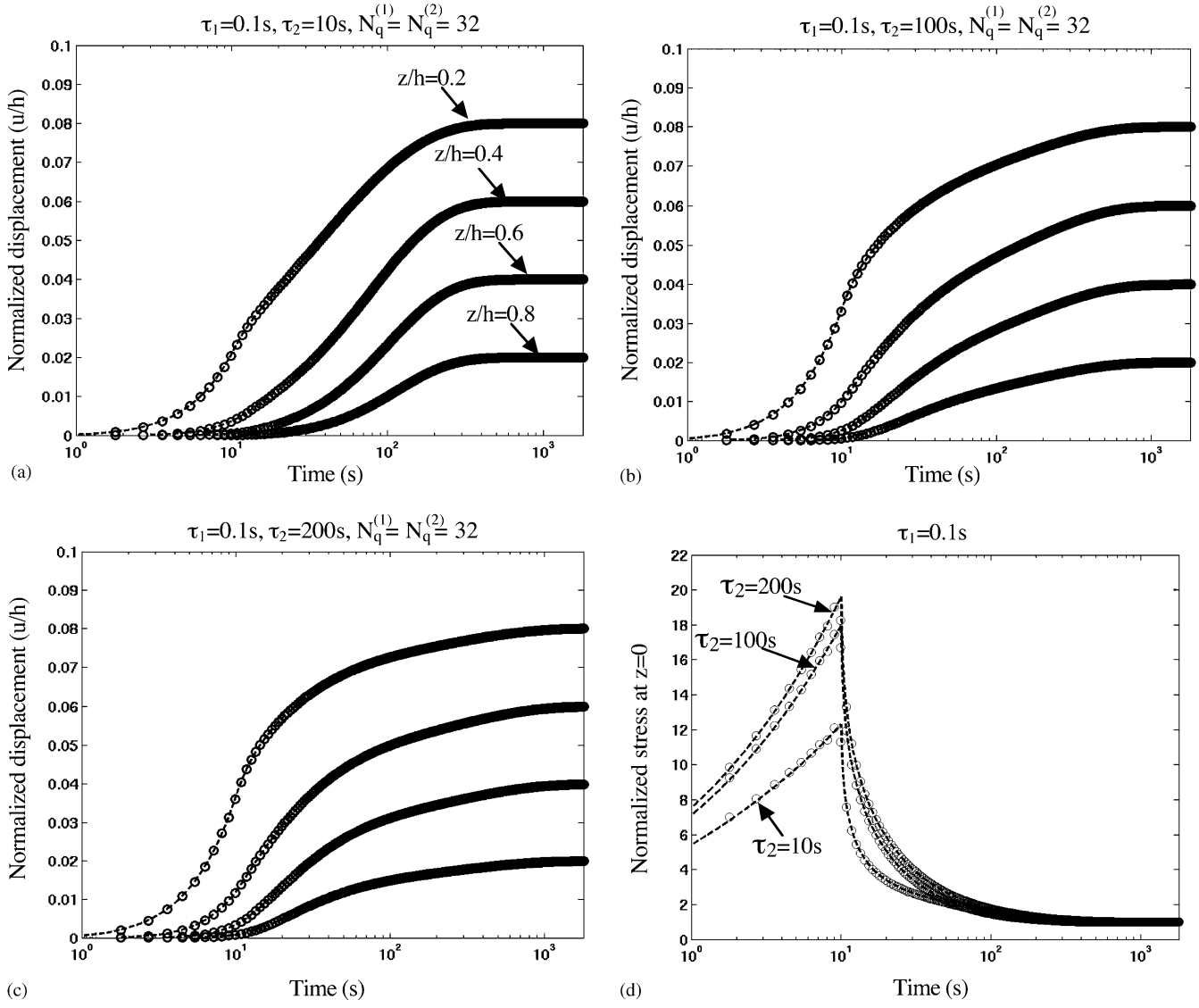

Fig. 3. Accuracy of the continuous spectrum BPVE numerical method ($\tau_1 = 0.1\,\text{s}, \Delta\bar{t} = \frac{1}{30}, \Delta\bar{z} = \frac{1}{20}$). The numerical solution (dashed) is compared to the theoretical solution (circles). Displacement profiles for the cases: (a) $\tau_2 = 10\,\text{s}$, (b) $\tau_2 = 100\,\text{s}$, (c) $\tau_2 = 200\,\text{s}$. (d) Surface stress with varying τ_2.

accurately reproduces the continuous spectrum relaxation model at the expense of additional storage requirements for the strain history, which must be retained for a period that is fixed, but not local, in time. For large applications, storage issues can be addressed by output of the strain history to an indexed file from which strain values at the quadrature abcissas can be rapidly extracted since their locations are determined by a simple coordinate transformation between the abcissas and the fixed time mesh on the truncated interval of integration. When $\bar{t} \gg \Delta\bar{t}$, the three strain values used in quadratic interpolation at an abcissa will remain unchanged for several steps in the time marching method, reducing the cost of file access.

The numerical method presented in this study will be useful in contexts where a discrete spectrum approximation is either undesirable or inaccurate. Applications include the experimental measurement of viscoelastic material parameters for articular cartilage, as well as more complex geometric simulations of tissue deformation for a fixed set of parameter values. While this study considered a finite difference solution of the 1D BPVE confined compression problem, our formulation can be extended to continuous spectrum viscoelastic models in higher dimensions. Specifically, in (4) the strain terms $\varepsilon(\bar{z}, \bar{t})$ and $\varepsilon(\bar{z}, \bar{\tau})$ can be replaced by the more general tensorial forms $\bar{\mathbf{S}}^e[\mathbf{e}(\bar{\mathbf{x}}, \bar{t})]$ and $\bar{\mathbf{S}}^e[\mathbf{e}(\bar{\mathbf{x}}, \bar{\tau})]$, respectively, where $\mathbf{e}$ is a strain tensor. In such an extended formulation, the modified kernel H in (5), and the analysis of time dependence based on its mathematical form, remain the same. Since the temporal and spatial dependence in (4) are uncoupled, the approach

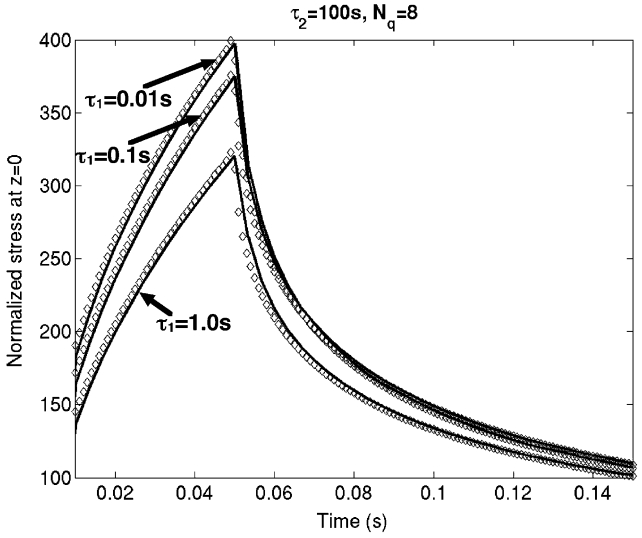

Fig. 4. Accuracy of the continuous spectrum BPVE numerical method for a high strain rate ($\Delta\bar{t} = \frac{1}{300}, \Delta\bar{z} = \frac{1}{80}$). The numerical solution (solid) is compared to the theoretical solution (diamonds) in the case $\tau_2 = 100$ s with varying τ_1.

presented in this study is, apparently, independent of the particular numerical method employed for spatial discretization. Since the method is based on Gaussian quadrature and interpolation, it can also be incorporated into variable time step numerical methods for solution of the governing momentum equation which would further increase computational efficiency. We also believe that this numerical method has the potential to significantly increase the efficiency of continuous spectrum BPVE FEMs.

Acknowledgements

This work has been supported by funding from the National Science Foundation (DMS-0211154).

References

Abramowitz, M., Stegun, I.A., 1972. Handbook of Mathematical Functions, ninth ed. Dover, New York.

deHoog, F.R., Knight, J.H., Stokes, A.N., 1982. An improved method for numerical inversion of Laplace transforms. SIAM Journal on Scientific and Statistical Computing 3, 357–366.

DiSilvestro, M.R., Suh, J.K., 2001. Cross-validation of the biphasic poroviscoelastic model of articular cartilage in unconfined compression, indentation and confined compression. Journal of Biomechanics 34, 519–525.

DiSilvestro, M.R., Suh, J.K., 2002. Biphasic poroviscoelastic characteristics of proteoglycan-depleted articular cartilage: simulation and degeneration. Annals of Biomedical Engineering 30, 792–800.

Fung, Y.C., 1993. Biomechanics: Mechanical Properties of Living Tissues, second ed. Springer, New York.

Hollenbeck, K.H., 1998. INVLAP.M: A matlab function for numerical inversion of Laplace transforms by the de Hoog algorithm. ftp://ftp.mathworks.com/pub/contrib/v5/math/invlap.m.

Mak, A.K., 1986. The apparent viscoelastic behavior of articular cartilage—the contributions from the intrinsic matrix viscoelasticity and interstitial fluid flows. Journal of Biomechanical Engineering 108, 123–130.

Mow, V.C., Kuei, S.C., Lai, W.M., Armstrong, C.G., 1980. Biphasic creep and stress relaxation of articular cartilage in compression: theory and experiments. Journal of Biomechanical Engineering 102, 73–84.

Neubert, H.K.P., 1963. A simple model representing internal damping in solid materials. Aeronautical Quarterly 14, 187–197.

Setton, L.A., Zhu, W., Mow, V.C., 1993. The biphasic poroviscoelastic behavior of articular cartilage: role of the surface zone in governing the compressive behavior. Journal of Biomechanics 26, 581–592.

Suh, J.K., Bai, S., 1998. Finite element formulation of biphasic poroviscoelastic model for articular cartilage. Journal of Biomechanical Engineering 120, 195–201.